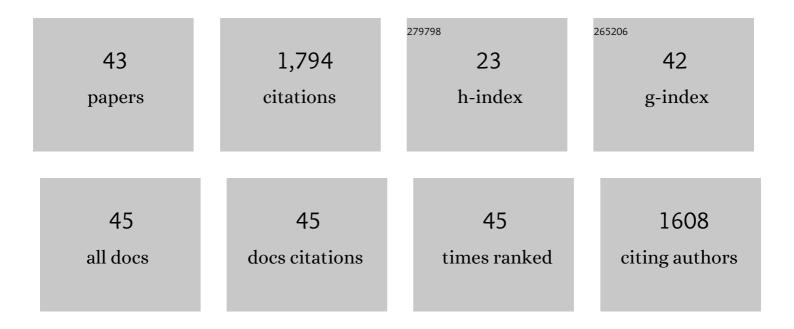
Javier Fullea

List of Publications by Year in descending order

Source: https://exaly.com/author-pdf/4553029/publications.pdf Version: 2024-02-01



INVIED FULLEN

#	Article	IF	CITATIONS
1	Effective elastic thickness of Africa and its relationship to other proxies for lithospheric structure and surface tectonics. Earth and Planetary Science Letters, 2009, 287, 152-167.	4.4	142
2	The structure and evolution of the lithosphere–asthenosphere boundary beneath the Atlantic–Mediterranean Transition Region. Lithos, 2010, 120, 74-95.	1.4	126
3	3â€D multiobservable probabilistic inversion for the compositional and thermal structure of the lithosphere and upper mantle. I: <i>a priori</i> petrological information and geophysical observables. Journal of Geophysical Research: Solid Earth, 2013, 118, 2586-2617.	3.4	121
4	FA2BOUG—A FORTRAN 90 code to compute Bouguer gravity anomalies from gridded free-air anomalies: Application to the Atlantic-Mediterranean transition zone. Computers and Geosciences, 2008, 34, 1665-1681.	4.2	116
5	LitMod3D: An interactive 3â€D software to model the thermal, compositional, density, seismological, and rheological structure of the lithosphere and sublithospheric upper mantle. Geochemistry, Geophysics, Geosystems, 2009, 10, .	2.5	107
6	A rapid method to map the crustal and lithospheric thickness using elevation, geoid anomaly and thermal analysis. Application to the Gibraltar Arc System, Atlas Mountains and adjacent zones. Tectonophysics, 2007, 430, 97-117.	2.2	106
7	The structure of the Atlantic–Mediterranean transition zone from the Alboran Sea to the Horseshoe Abyssal Plain (Iberia–Africa plate boundary). Marine Geology, 2007, 243, 97-119.	2.1	82
8	3â€D multiâ€observable probabilistic inversion for the compositional and thermal structure of the lithosphere and upper mantle. II: General methodology and resolution analysis. Journal of Geophysical Research: Solid Earth, 2013, 118, 1650-1676.	3.4	78
9	3â€D multiobservable probabilistic inversion for the compositional and thermal structure of the lithosphere and upper mantle: III. Thermochemical tomography in the Westernâ€Central U.S Journal of Geophysical Research: Solid Earth, 2016, 121, 7337-7370.	3.4	67
10	Electrical conductivity of continental lithospheric mantle from integrated geophysical and petrological modeling: Application to the Kaapvaal Craton and Rehoboth Terrane, southern Africa. Journal of Geophysical Research, 2011, 116, .	3.3	66
11	Water in cratonic lithosphere: Calibrating laboratoryâ€determined models of electrical conductivity of mantle minerals using geophysical and petrological observations. Geochemistry, Geophysics, Geosystems, 2012, 13, .	2.5	63
12	Lithospheric structure of the Gorringe Bank: Insights into its origin and tectonic evolution. Tectonics, 2010, 29, n/a-n/a.	2.8	53
13	Lithospheric structure in the Baikal–central Mongolia region from integrated geophysicalâ€petrological inversion of surfaceâ€wave data and topographic elevation. Geochemistry, Geophysics, Geosystems, 2012, 13, .	2.5	53
14	Seismic tomography of the Arctic region: inferences for the thermal structure and evolution of the lithosphere. Geological Society Special Publication, 2018, 460, 419-440.	1.3	52
15	WINTERC-G: mapping the upper mantle thermochemical heterogeneity from coupled geophysical–petrological inversion of seismic waveforms, heat flow, surface elevation and gravity satellite data. Geophysical Journal International, 2021, 226, 146-191.	2.4	49
16	Integrated geophysical-petrological modeling of lithosphere-asthenosphere boundary in central Tibet using electromagnetic and seismic data. Geochemistry, Geophysics, Geosystems, 2014, 15, 3965-3988.	2.5	40
17	Lithospheric structure in the Atlantic–Mediterranean transition zone (southern Spain, northern) Tj ETQq1 1 2006, 338, 140-151.	0.784314 rg 1.2	gBT /Overlock 38
18	The Canary Islands hot spot: New insights from 3D coupled geophysical–petrological modelling of the lithosphere and uppermost mantle. Earth and Planetary Science Letters, 2015, 409, 71-88.	4.4	37

JAVIER FULLEA

#	Article	IF	CITATIONS
19	Integrated geophysical modelling of a lateral transition zone in the lithospheric mantle under Norway and Sweden. Geophysical Journal International, 2013, 194, 1358-1373.	2.4	32
20	Velocityâ€conductivity relations for cratonic lithosphere and their application: Example of Southern Africa. Geochemistry, Geophysics, Geosystems, 2013, 14, 806-827.	2.5	31
21	The lithosphere–asthenosphere system beneath Ireland from integrated geophysical–petrological modeling II: 3D thermal and compositional structure. Lithos, 2014, 189, 49-64.	1.4	31
22	Decoupled crust-mantle accommodation of Africa-Eurasia convergence in the NW Moroccan margin. Journal of Geophysical Research, 2011, 116, .	3.3	30
23	Perturbing effects of sub-lithospheric mass anomalies in GOCE gravity gradient and other gravity data modelling: Application to the Atlantic-Mediterranean transition zone. International Journal of Applied Earth Observation and Geoinformation, 2015, 35, 54-69.	2.8	27
24	Shearâ€Wave Velocity Structure of Southern Africa's Lithosphere: Variations in the Thickness and Composition of Cratons and Their Effect on Topography. Geochemistry, Geophysics, Geosystems, 2018, 19, 1499-1518.	2.5	24
25	Hot Upper Mantle Beneath the Tristan da Cunha Hotspot From Probabilistic Rayleighâ€Wave Inversion and Petrological Modeling. Geochemistry, Geophysics, Geosystems, 2018, 19, 1412-1428.	2.5	23
26	Constraining the geotherm beneath the British Isles from Bayesian inversion of Curie depth: integrated modelling of magnetic, geothermal, and seismic data. Solid Earth, 2019, 10, 839-850.	2.8	23
27	The lithosphere–asthenosphere system beneath Ireland from integrated geophysical–petrological modeling — I: Observations, 1D and 2D hypothesis testing and modeling. Lithos, 2014, 189, 28-48.	1.4	22
28	Geochemical and geophysical constrains on the dynamic topography of the <scp>S</scp> outhern <scp>A</scp> frican <scp>P</scp> lateau. Geochemistry, Geophysics, Geosystems, 2017, 18, 3556-3575.	2.5	20
29	On Joint Modelling of Electrical Conductivity and Other Geophysical and Petrological Observables to Infer the Structure of the Lithosphere and Underlying Upper Mantle. Surveys in Geophysics, 2017, 38, 963-1004.	4.6	18
30	Lithospheric structure of Central Europe: Puzzle pieces from Pannonian Basin to Transâ€European Suture Zone resolved by geophysicalâ€petrological modeling. Tectonics, 2016, 35, 722-753.	2.8	17
31	Geodynamic Modeling of Edge-Delamination Driven by Subduction-Transform Edge Propagator Faults: The Westernmost Mediterranean Margin (Central Betic Orogen) Case Study. Frontiers in Earth Science, 2020, 8, .	1.8	12
32	3-D thermochemical structure of lithospheric mantle beneath the Iranian plateau and surrounding areas from geophysical–petrological modelling. Geophysical Journal International, 2020, 222, 1295-1315.	2.4	12
33	On the origin of the Canary Islands: Insights from mantle convection modelling. Earth and Planetary Science Letters, 2022, 584, 117506.	4.4	12
34	Integrating Gravity and Surface Elevation With Magnetic Data: Mapping the Curie Temperature Beneath the British Isles and Surrounding Areas. Frontiers in Earth Science, 2018, 6, .	1.8	9
35	A refined model of sedimentary rock cover in the southeastern part of the Congo basin from GOCE gravity and vertical gravity gradient observations. International Journal of Applied Earth Observation and Geoinformation, 2015, 35, 70-87.	2.8	8
36	The topography of the Iberian Peninsula from integrated geophysical-petrological multi-data inversion. Physics of the Earth and Planetary Interiors, 2021, 314, 106691.	1.9	6

JAVIER FULLEA

#	Article	IF	CITATIONS
37	Comment on "Deep resistivity cross section of the intraplate Atlas Mountains (NW Africa): New evidence of anomalous mantle and related Quaternary volcanismâ€: Tectonics, 2012, 31, .	2.8	4
38	Probabilistic Surface Heat Flow Estimates Assimilating Paleoclimate History: New Implications for the Thermochemical Structure of Ireland. Journal of Geophysical Research: Solid Earth, 2018, 123, 10,951.	3.4	4
39	Benchmark forward gravity schemes: the gravity field of a realistic lithosphere model WINTERC-G. Solid Earth, 2022, 13, 849-873.	2.8	4
40	Longâ€Wavelength Gravity Field Constraint on the Lower Mantle Viscosity in North America. Journal of Geophysical Research: Solid Earth, 2020, 125, e2020JB020484.	3.4	2
41	A new integrated geophysical-petrological global 3-D model of upper-mantle electrical conductivity validated by the Swarm <i>M</i> 2 tidal magnetic field. Geophysical Journal International, 2021, 226, 742-763.	2.4	2
42	Inversion of the satellite observations of the tidally induced magnetic field in terms of 3-D upper-mantle electrical conductivity: method and synthetic tests. Geophysical Journal International, 2022, 229, 2115-2132.	2.4	1
43	Towards a Digital Twin of the Earth System: Geo-Soft-CoRe, a Geoscientific Software & Code Repository. Frontiers in Earth Science, 2022, 10, .	1.8	1